Bioorganic & Medicinal Chemistry 20 (2012) 5583–5591

Contents lists available at SciVerse ScienceDirect

Bioorganic & Medicinal Chemistry

journal homepage: www.elsevier.com/locate/bmc

Design of potent bisphosphonate inhibitors of the human farnesyl pyrophosphate synthase via targeted interactions with the active site 'capping' phenyls

Joris W. De Schutter [a], Joseph Shaw [b,†], Yih-Shyan Lin [a], Youla S. Tsantrizos [a,b,*]

[a] Department of Chemistry, McGill University, 801 Sherbrooke Street West, Montreal, QC, Canada H3A 0B8
[b] Department of Biochemistry, McGill University, 3649 Promenade Sir William Osler, Montreal, QC, Canada H3G 0B1

ARTICLE INFO

Article history:
Received 22 May 2012
Revised 4 July 2012
Accepted 13 July 2012
Available online 24 July 2012

Keywords:
Nitrogen-containing bisphosphonates
Farnesyl pyrophosphate synthase

ABSTRACT

Nitrogen-containing bisphosphonates (*N*-BPs) are potent active site inhibitors of the human farnesyl pyrophosphate synthase (hFPPS) and valuable human therapeutics for the treatment of bone-related malignancies. *N*-BPs are also useful in combination chemotherapy for patients with breast, prostate and multiple myeloma cancers. A structure-based approach was employed in order to design inhibitors that exhibit higher lipophilicity and better occupancy for the GPP sub-pocket of hFPPS than the current therapeutic drugs. These novel analogs were designed to bind deeper into the GPP sub-pocket by displacing the side chains of the 'capping' residue Phe 113 and engaging in favorable π-interactions with the side chain of Phe112.

1. Introduction

Human farnesyl pyrophosphate synthase (hFPPS) occupies the first branching point of the mevalonate pathway and catalyzes the sequential elongation of dimethylallyl pyrophosphate (DMAPP) to geranyl pyrophosphate (GPP) and then to farnesyl pyrophosphate (FPP), via sequential condensation of isopentenyl pyrophosphate (IPP) units. Consequently, hFPPS also controls intracellular levels of all isoprenoid metabolites and modulates the post-translational prenylation of the Ras family of GTPases (e.g., H-Ras, K-Ras, N-Ras) that are essential for cell survival.[1] It is well established that mutated Ras proteins are predominant in oncogenesis,[1] prompting the development of farnesyltransferase (FTase) inhibitors (FTI) as potential therapeutics for the treatment of cancer.[1] Despite the promising in vitro and preclinical efficacy of these inhibitors, only a small subset of patients responded to FTI therapy, leading to the realization that in vivo inhibition of farnesylation induces geranylgeranylation of the mutated Ras proteins, restoring their biological function. This redundancy mechanism suggests that upstream direct inhibition of FPP biosynthesis may be more effective in reducing Ras prenylation than inhibition of the FTase enzyme.

Currently, nitrogen-containing bisphosphonates (*N*-BPs; Fig. 1), such as zoledronate (**1**) and risedronate (**2a**), are the only class of clinically validated drugs that target the human FPPS.[2,3] Recent pre-clinical and clinical investigations have provided evidence for multiple mechanisms that mediate *N*-BP-induced antitumor effects, including apoptotic cell death, cell cycle disruption and γδ T cell activation.[4,5] *N*-BP-induced inhibition of cell proliferation and apoptosis has been reported in prostate,[6] and breast cancer,[7,8] multiple myeloma cells,[9,10] and other types of cancers. The apoptotic effects of *N*-BPs has been correlated with the intracellular accumulation of IPP (as a consequence of the hFPPS inhibition) and the formation of an ATP derivative (ApppI),[4,5] which inhibits the mitochondrial adenine nucleotide translocase and induces apoptosis. Additionally, IPP is a natural antigen of γδ T cells that is recognized by human Vγ2 Vδ2-bearing T cells (alternate nomenclature Vγ9 Vδ2).[11] During tumor invasion (or infection), γδ T cells expressing Vγ2 Vδ2 T-cell antigen receptors (TCRs) expand to high levels and, in some cases, they can represent the majority of circulating T cells. Short hairpin RNA-mediated knockdown of hFPPS in hematopoietic and non-hematopoietic tumor cell lines has been shown to activate Vγ2 Vδ2 T cells and induce IFN-γ secretion.[12] Evidence for the stimulation of Vγ2 Vδ2-bearing T cells by *N*-BPs has been observed in multiple myeloma patients treated with pamidronate (**3**)[13] and prostate cancer patients treated with zoledronate (**1**);[6] in the latter case, the observed γδ T cell stimulation coincided with reduction in serum prostate-specific antigen (PSA), providing further evidence of an antitumor immune response that is induced by *N*-BPs in vivo. Interestingly, although good correlation between hFPPS inhibition and γδ T cell activation has been observed, *N*-BPs that target other closely related enzymes, such as the human geranylgeranyl pyrophosphate synthase (hGGPPS; e.g., compound **5**) or the human undecaprenyl

* Corresponding author. Tel.: +1 514 398 3638; fax: +1 514 398 3797.
E-mail address: youla.tsantrizos@mcgill.ca (Y.S. Tsantrizos).
† Undergraduate research participant

0968-0896/$ - see front matter © 2012 Elsevier Ltd. All rights reserved.
http://dx.doi.org/10.1016/j.bmc.2012.07.019

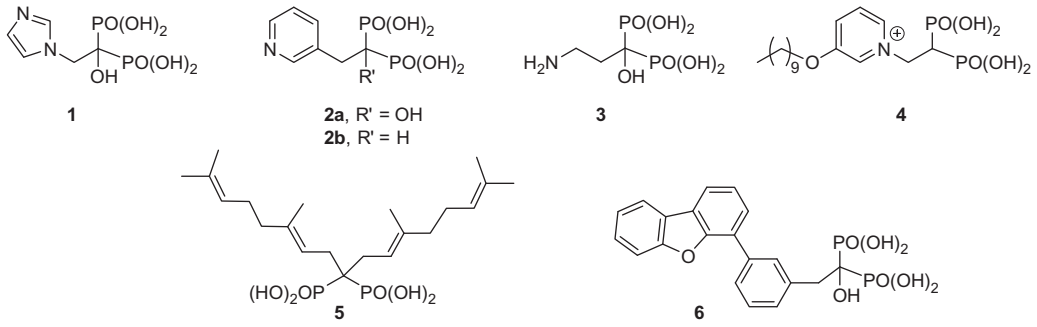

Figure 1. Examples of known *N*-BPs that inhibit hFPPS, hGGPPS or *E. coli* UPPS.

pyrophosphate synthase (hUPPS; e.g., compound **6**) do not induce γδ T cell activation.[14,15]

The structural features and physicochemical properties of the current *N*-BP drugs (e.g., **1** and **2a**) limit their therapeutic use to bone-related diseases, due to their high affinity for bone, poor oral bioavailability, very low cell membrane permeability and negligible distribution into non-skeletal tissues.[16] Therefore, the identification of more lipophilic, potent and selective inhibitors of hFPPS is of considerable interest. Recently, we reported the design of novel lead structures that bind to a larger portion of the active site cavity of hFPPS than the current drugs **1** and **2a** and are also more lipophilic.[17] In this report, we describe our subsequent efforts in exploring the interactions between these inhibitors and the GPP sub-pocket of the hFPPS active site.

2. Results

2.1. Chemistry

The synthesis of novel *N*-BPs is outlined in Schemes 1 and 2. Analogs **7** and **8** were synthesized as previously reported.[17] The synthesis of analogs **9** was initiated by the condensation of 5-bromopyridin-3-amine (**11**) with triethyl orthoformate and diethylphosphite at 100 °C to give the bisphosphonate tetraethyl ester **12** in moderate yield (~45% isolated yield; Scheme 1). We noted that this condensation leads to significant decomposition if carried out at 120 °C, whereas at 80 °C the reaction proceeds very slowly. Suzuki cross-coupling of intermediate **12** with the boronic acids or boronate esters of fragments shown in Table 1 provided the biaryl intermediates **13** in variable yields (35–99% isolated yields). Deprotection of the bisphosphonate tetraesters was achieved after treatment with TMSBr, followed by methanolysis and trituration to give the final *N*-BP inhibitors of general structure **9** (Scheme 1; Table 1).

Condensation of intermediate **12** with benzyl potassium trifluoroborate, as previously described by Molander,[18] provided the tetraethyl ester precursor to analog **9c**. The boronate reagent of fragment **g** was prepared via cyclopropanation of the precursor vinyl ether using Simmons–Smith-type conditions with TFA as an additive.[19] Details on the synthesis of all non-commercial boronate reagents are described in the supporting information.

Preparation of analogs **10** originated from 4-carboxypyridine-1-oxide (**14**) which was first converted to the methyl ester, with MeOH under acid conditions and azeotropic dehydration (Scheme 2). The pyridine N-oxide ester was subsequently converted to the corresponding 2-aminopyridine **15** using *t*-BuNH$_2$ and tosyl anhydride as the activating reagent, followed by removal of the *t*-butyl group with TFA.[20] Conversion of the aniline to the bisphosphonate tetraesters **16a** was achieved using previously reported conditions.[17] Saponification of the methyl esters **16a** to the corresponding acid (**16b**) was performed at 0 °C in order to prevent partial deprotection of the tetraethyl bisphosphonate esters. Amide bond formation was catalyzed by HATU and the final bisphosphonic acids were obtained after treatment with TMSBr followed by methanolysis and trituration to give the final *N*-BPs of general structure **10** (Scheme 2).

2.2. Biological data and discussion

2.2.1. Human FPPS inhibition and SAR

Inhibition of the human recombinant enzymes FPPS (hFPPS) and GGPPS (hGGPPS) were determined using the in vitro assays described previously.[17,21] For efficiency, all compounds were initially tested at a single concentration of 1 μM and only those analogs exhibiting greater than 80% inhibition at 1 μM (average of triplicate determinations; standard deviation of <10%) were profiled further to determine their IC$_{50}$ values (Table 2). Representative examples were also evaluated of their ability to inhibit the structurally and functionally related enzyme hGGPPS.

Recently, we reported the co-crystal structure of analog **7f** which binds deeper into the GPP sub-pocket of the hFPPS active site than the clinical drugs **1** and **2a**.[17] In the hFPPS/**7f** complex, the pyridine nitrogen of the inhibitor participates in a H$_2$O-mediated hydrogen-bond interactions with the side chain carbonyl oxygen of Gln 254. In contrast, the heterocyclic side chains of **1** and **2a** form bifurcated hydrogen-bonds with the amide carbonyl of Lys 200 and the side chain oxygen of Thr 201.[2,3] These hydrogen-bonds play a significant role in the potency of **1** and **2a** in inhibiting hFPPS. For example, a >280-fold loss in potency has been observed when the pyridine side chain of **2a** is replaced by a simple phenyl ring.[22] Superposition of the co-crystal structures of hFPPS/**2a** (PDB: 1YV5) and hFPPS/**7f** (PDB: 4DEM) revealed that the pyridine rings

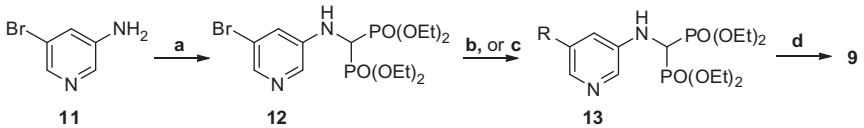

Scheme 1. Reagents and conditions: (a) HP(O)(OEt)$_2$, CH(OEt)$_3$, toluene, 100 °C; (b) boronic acid, Pd(PPh$_3$)$_4$, 2 M K$_2$CO$_3$, dioxane, μW 125 °C (~40 W); (c) benzyl potassium trifluoroborate, Pd(dppf)Cl$_2$·CH$_2$Cl$_2$, Cs$_2$CO$_3$, dioxane, μW 125 °C (~40 W); (d) (i) TMSBr, DCM; (ii) MeOH.

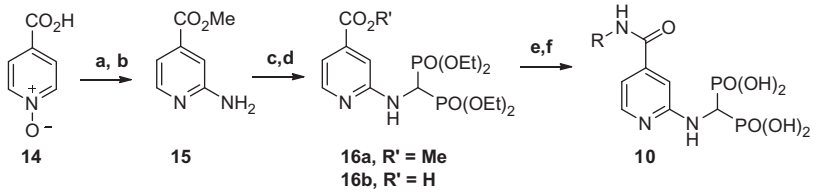

Scheme 2. Reagents and conditions: (a) cat. H_2SO_4, MeOH, toluene, reflux, Dean–Stark; (b) (i) Ts_2O, $CHCl_3$, 0 °C; (ii) *t*-$BuNH_2$, (iii) TFA, 70 °C; (c) $HP(O)(OEt)_2$, $CH(OEt)_3$, toluene, 120 °C, overnight; (d) LiOH, THF/H_2O, 0 °C; (e) RNH_2, HATU, DIPEA, DMF; (f) (i) TMSBr, DCM; (ii) MeOH.

Table 1
Novel *N*-BP inhibitors.

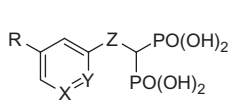

7, X = CH_2, Y = N, Z = NH, R = a-j
8, X = N, Y = CH, Z = CH_2, R = a-j
9, X = N, Y = CH, Z = NH, R = a-j

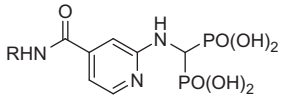

10, R = a-j

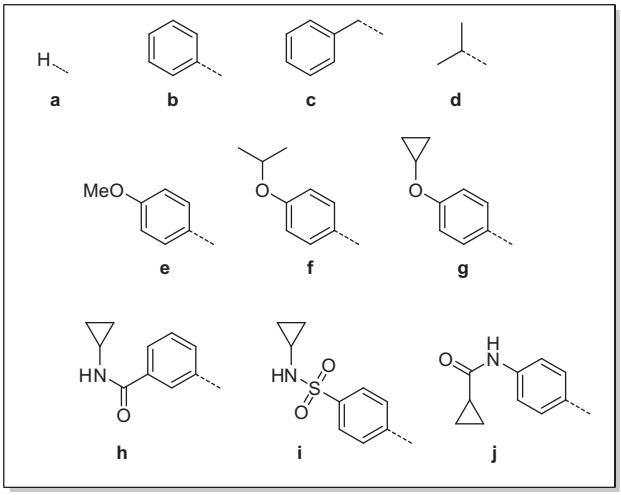

Table 2
Inhibition data for hFPPS

Compound	hFPPS IC_{50} (nM)	SASA[e]	FISA[e]
2a[a]	11	433	262
7a[b]	85	427	239
7b[b]	150	548	238
7e[b]	115	562	238
7f[a]	28	624	238
7g[a]	12	638	238
8b[a]	164	544	239
9b[a]	47	542	250
9c[a]	~1000[c]	558	251
9f[a]	60	618	251
9g[a]	16	632	251
9h[a]	IN	661	288
9i[a]	IN	671	317
9j[a]	>1000[d]	663	291
10b[a]	IN	594	281
10d[a]	~1000[c]	570	276
10e[a]	IN	609	281

[a] Compound exhibited less than 50% inhibition in the hGGPPS enzymatic assay at 10 μM.
[b] Compound was not tested in the hGGPPS enzymatic assay.
[c] 55–65% inhibition at 1 μM.
[d] 40% inhibition at 1 μM; IN = inactive at 1 μM.
[e] Calculated using QikProp 3.2; SASA = total solvent accessible surface area in A^2 using a probe with 1.4 A radius; FISA = hydrophilic component of SASA.

of both inhibitors overlapped in their hFPPS-bound conformations (Fig. 2). However, the pyridine nitrogen of **2a** (which is at the *meta*-position relative to the C-β of the bisphosphonate moiety) could more easily engage in bifurcated hydrogen-bond interactions with Lys 200 and Thr 201 than analog **7f**. We presumed that the loss of interactions between pyridine side chain and the Lys 200/Thr 201 residues may be (in part) the reason for the lower in vitro potency of analogs with general structure **7** as compared to **2a** (e.g., **7a** is approximately eightfold less potent than **2a**, under our assay conditions; Table 2). However, we observed that analogs **7b** and **8b** are almost equipotent (Table 2). Although the reasons for these results are not clearly apparent, a possible explanation may be that the higher acidity of a Cα-amino bisphosphonate (i.e., **7b**) may compensate for the loss of H-bond interactions between the side chains of analogs **7** and Lys 200/Thr 201. Consistent with the latter assumption, a threefold increase in potency was observed for analog **9b** as compared to **7b** (Table 2). The overall sp^2 character of the exocyclic amine linker (via conjugation of its lone-pair of electrons with the aromatic ring) may also contribute to the stabilization of the bioactive conformation of analogs **7** and **9**, in which the Cα of the bisphosphonate moiety is nearly co-planar (<10° out of plane) with respect to the pyridine core.

In the co-crystal structure of the hFPPS-bound **7f**, the 4-isopropoxyphenyl side-chain is almost co-planar with the pyridine ring and inserted between the side chains of Phe 113 and Gln 185,

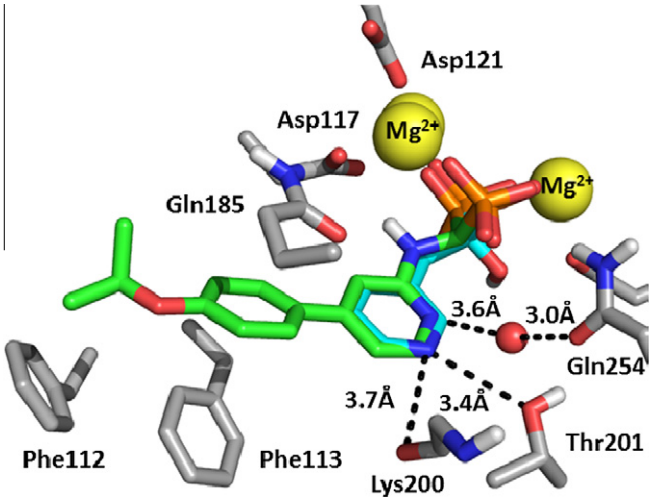

Figure 2. Superposition of X-ray structures of *N*-BPs bound to the active site of hFPPS, with the bound inhibitors and key residues shown in stick form. The carbon backbone of **2a** is highlighted in cyan, and **7f** in green. Oxygen, nitrogen and phosphorus atoms are coloured in red, blue and orange, respectively. The yellow spheres represent the Mg^{2+} ions. The bifurcated H-bonds of **2a** with the backbone carbonyl of Lys 200 and the side chain hydroxyl of Thr 201 are highlighted with dashed lines; similarly, the water (red sphere) mediated H-bond of the pyridine nitrogen of **7f** with Gln 254 is also indicated. The phenyl moiety of the 4-isopropoxyphenyl side chain of **7f** is 'stacked' between the side chains of Phe 113 and Gln 185.

engaging in stacking interactions (Fig. 2). In an effort to optimize these interactions, a number of derivatives were synthesized varying the electronic character and conformation of the—R substituent in analogs **7**, **8**, **9** and **10**. Disruption of the co-planarity between the side chain pyridine moiety and the—R substituent by the introduction of a simple methylene linker resulted in greater than 20-fold loss in potency (e.g., analogs **9b** vs **9c**; Table 2). We expected that an amide bond would maintain the overall co-planarity of the side chain and engage in favorable π-stacking interactions with Phe 113. However, the introduction of such a linker was equally detrimental to the potency of these compounds (e.g., IC_{50} of **9b** vs **10b**; Table 2). A number of other modifications were also evaluated, including analogs with small side chains (e.g., **10d**) and all were found to be detrimental. Based on these results, we concluded that a direct aryl–aryl bond between the pyridine core and aromatic side chain is best suited to occupy the extended lipophilic channel formed upon binding of inhibitor **7f** to the GPP subpocket. It is also possible that this lipophilic channel does not tolerate binding of polar groups, such as an amide moiety.

In addition to the stacking interactions of the 4-isopropoxyphenyl moiety of **7f** with the side chains of Phe 113 and Gln 185 (Fig. 2), we also observed that the isopropyl substituent was protein-bound within Van der Waals distance from the aromatic side chain of Phe 112. Our SAR studies also suggested favorable interactions between the inhibitor side chain and Phe 112. For example, the methoxy derivative **7e** was only slightly more potent than **7b**, whereas analog **7f** was approximately fivefold more potent than **7b** (Table 2). Consequently, we assumed that the corresponding cyclopropyl analog **7g** could further increase interactions with the aromatic ring of Phe 112 via CH/π-interactions (due to the inherent π-character of the C–C bonds in the cyclopropyl ring). Indeed, this minor modification improved the enzymatic potency approximately threefold in series **7** and approximately fourfold in series **9** (e.g., **7f** vs **7g** and **9f** vs **9g**, respectively; Table 2). Consistent with our prediction, in silico docking (using GLIDE) of **7g** indicated that the carbon atoms of the cyclopropyl ring would bind with a ~3.4 Å distance from the aromatic ring of Phe 112, allowing for favorable CH/π-interaction (Fig. 3).[23–26]

We also explored different linkers between the phenyl sidechain and the cyclopropyl moiety of inhibitor **9g**. We noted that in the co-crystal structure of the hFPPS/**7f** the isopropyl moiety is partly solvent exposed, consequently, we decided to introduce a polar linker, including an amide, a reversed amide and a sulfonamide, that could perhaps orient the cyclopropyl moiety more favorably towards the aromatic side chain of Phe 112. Unfortunately, all these analogs (e.g., **9h**, **9i** and **9j**) proved to be significantly less potent than **9g**, leading to less than 50% inhibition of hFPPS at even 1 μM concentration of inhibitor (Table 1).

Many of these analogs were also tested in our enzymatic assay using the related human enzyme GGPPS and found to exhibit less than 50% inhibition at 10 μM concentration (Table 2). This observed selectivity is uncommon for *N*-BP compounds that have larger side chains, such as compound **4**, which is a dual inhibitor of hFPPS and hGGPPS (with IC_{50} values of 100 and 280 nM, respectively)[14] and compound **5** which inhibits only hGPPS (an IC_{50} value of 410 nM was determined under our assay conditions).

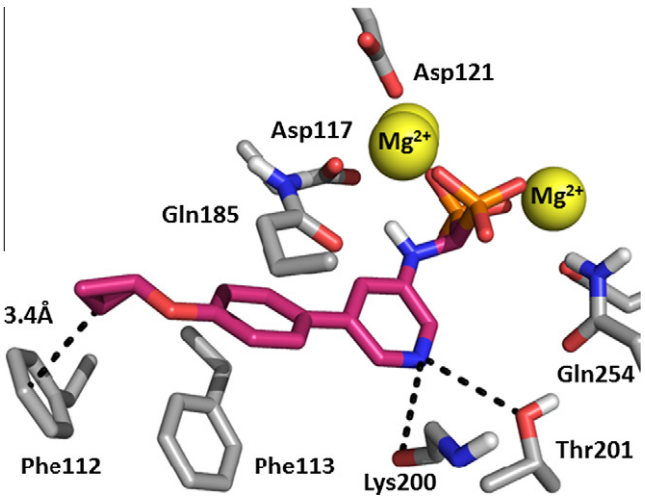

Figure 3. Docking output structure of inhibitor **9g** (using GLIDE version 5.5, Shrödinger, LLC, New York, NY 2009; standard parameters of XP-mode were used) in the hFPPS/**7f** co-crystal structure (PDB: 4DEM). The predicted bifurcated H-bond and cyclopropyl-π interactions are indicated with dashed lines.

3. Conclusion

The current *N*-BP drugs exhibit poor cell-membrane permeability and bind so avidly to bone that their penetration into non-skeletal tissues is practically negligible. The Cα-hydroxybisphosphonate moiety is the main pharmacophore anchoring these drugs to the active site of hFPPS, via chelation of three Mg^{2+} ions that also interact with highly conserved aspartic acid residues within the GPP sub-pocket of the active site cavity. In spite numerous efforts from both academic and industrial research group, to date, the identification of highly potent and selective inhibitors of hFPPS, with low affinity for bone, and sufficiently high cell membrane permeability to provide good exposure of the drug in non-skeletal tissues, remains a huge challenge.

The active site occupancy of the enzyme-bound current drugs (e.g., **1** and **2a**) is hugely suboptimal, leaving a large portion of the cavity unoccupied. Based on this knowledge, we focused our efforts in designing *N*-BP analogs that have a more optimal shape, size and electrostatic surface complementarity with the hFPPS active site, lower affinity for bone and increased lipophilicity. We began our studies with the virtual screening of over 1000 pyridine-based compounds, using docking calculations.[21] However, the correlation between our in silico predictions and the experimental data was generally poor;[17] this observation is not unexpected, given the high protein plasticity of hFPPS. Nonetheless, in silico docking provided some reassurance in guiding the design of analogs with very conservative structural variations and based on the X-ray structure of our lead compound **7f**.[17] For example, the design of the cyclopropoxy derivatives **7g** and **9g** (IC_{50} values of 12 and 16 nM, respectively) were based on the co-crystal structure of **7f** (IC_{50} = 28 nM).

In summary, as part of our lead optimization efforts, we synthesized analogs that are able to induce conformational changes to the active site cavity, enlarge the available binding space within the GPP sub-pocket by displacing the side chains of the Phe 113 and Gln 185 and engage in novel interactions with Phe 112. In contrast to previously reported *N*-BPs that have a large side chain (e.g., **4**, **5** and **6**) and poor ability to inhibit hFPPS, compounds **7f**, **7g** and **9g** exhibit an unusually high selectivity in inhibiting hFPPS versus hGGPPS; the latter enzyme represents the most closely related human enzyme. Furthermore, the relative hydrophobicity of our most potent analogs **7f**, **7g**, **9g** is significantly higher than that of the drug risedronate (**2a**), as estimated by the % hydrophilic component of the total solvent accessible surface area of each molecule in $Å^2$ (Table 2; calculations were carried out using QuikProp and a probe with 1.4 Å radius). For example, the% hydrophilic component (out of the total surface area) of **2a** is approximately 61% as compared to 38–40% for inhibitors **7f**, **7g**, **9g**. These novel compounds represent promising leads towards the identification of potent and selective hFPPS inhibitors with better biopharmaceutical properties than the current drugs.

4. Experimental

4.1. General procedures for characterization of compounds

All intermediate compounds were purified by normal phase flash column chromatography on silica gel using a CombiFlash instrument and the solvent gradient indicated. The purified bisphosphonate tetra ester precursors of all final inhibitors were analyzed by reverse-phase HPLC and fully characterized by ^{1}H, ^{13}C and ^{31}P NMR, and MS. The homogeneity of the bisphosphonate tetra esters (>90%) was confirmed by C18 reversed phase HPLC, using Method A indicated below. After ester hydrolysis, the final bisphosphonic acid products were precipitated and washed with deionized H_2O, HPLC grade acetonitrile and distilled Et_2O to obtain the inhibitors as white solids; quantitative conversion of each tetra ester to the corresponding bisphosphonic acid was confirmed by ^{31}P NMR. All final products were characterized by ^{1}H, ^{13}C, ^{31}P and ^{19}F NMR and HR-MS. Chemical shifts (δ) are reported in ppm relative to the internal deuterated solvent (^{1}H, ^{13}C) or external H_3PO_4 (δ 0.00 ^{31}P), unless indicated otherwise. Low- and High-Resolution MS spectra were recorded at the McGill University, MS facilities using electrospray ionization ($ESI^{\pm}$). The homogeneity of the final inhibitors was confirmed by HPLC using Method B (indicated below). Only samples with >95% homogeneity were tested in the enzymatic assays for the determination of IC_{50} values. HPLC Analysis was performed using a Waters ALLIANCE® instrument (e2695 with 2489 UV detector and 3100 mass spectrometer).

4.1.1. HPLC sample preparation

A precise amount of bisphosphonate inhibitor was weighed out, suspended in Milli-Q grade water and dissolved by the addition of 1–4 equiv of a 1.030 M standardized NaOH solution. The samples were then diluted to 1 or 2 mM concentration and 10 μl was injected for HPLC analysis.

Method A: Waters Atlantis T3 C18 5 μm

Solvent A: H_2O, 0.1% formic acid

Solvent B: CH_3CN, 0.1% formic acid

Mobile phase: linear gradient from 95%A and 5%B to 5%A and 95%B in 13 min, then 2 min at 100% B

Flow rate: 1 mL/min

Method B: Waters XSELECT CSH fluoro-phenyl, 5 μm column

Solvent A: H_2O, 0.06% TFA

Solvent B: CH_3CN, 0.06% TFA

Mobile phase: linear gradient from 99%A, 1%B to 100%B in 10 min, then 5 min at 100% B

4.2. Synthesis of methyl 2-aminoisonicotinate (15)

Isonicotinic acid *N*-oxide (3.00 g, 21.6 mmol) was dissolved in 20 ml 1:1 methanol/toluene, a catalytic amount H_2SO_4 was added and the flask was equipped with a Dean Stark trap filled with toluene. The mixture was refluxed overnight. The reaction was terminated by cooling in an ice bath, and neutralized with satd. sodium carbonate. The solution was extracted using (5 × 20 ml) DCM; the organic phases were combined, washed with brine, dried with $MgSO_4$, filtered and concentrated in vacuo. The residue was purified by silica gel chromatography using a CombiFlash instrument and a solvent gradient from 100% hexanes to 100% EtOAc to give 4-(methoxycarbonyl) pyridine 1-oxide as a white powder (1.46 g, 45%). ^{1}H NMR (300 MHz, $CDCl_3$) δ 8.24–8.16 (m, 2H), 7.93–7.79 (m, 2H), 3.94 (s, 3H).

To an ice-cooled solution of the above product (4-(methoxycarbonyl)pyridine 1-oxide, 300 mg, 1.96 mmol) in $CHCl_3$ was added tosyl anhydride (2877 mg, 8.82 mmol) and the mixture was stirred for 5 min. Next, *t*-$BuNH_2$ (1.24 ml, 11.8 mmol) was added dropwise via syringe to the activated N-oxide while maintaining the reaction temperature below 5 °C. The reaction was monitored by TLC and until complete consumption of starting material (~30 min) was observed. TFA (10.0 ml, 131 mmol) was added to the reaction mixture and the reaction was stirred at 70 °C overnight. The mixture was diluted with water (5 mL) and DCM (10 mL) and carefully neutralized with saturated $NaHCO_3$. The aqueous layer was extracted using DCM (4 × 10 mL). The combined organic layers were washed once with brine, dried over $MgSO_4$, filtered and concentrated in vacuo. The residue was purified by silica gel chromatography using a CombiFlash instrument and a solvent gradient from 100% hexanes to 100% EtOAc and then to 25% MeOH in EtOAc (all eluents contained 0.1% triethylamine) to yield the desired methyl 2-aminoisonicotinate product obtained as reddish/brown crystals (153.3 mg, 51%). ^{1}H NMR (400 MHz, $CDCl_3$) δ 8.19 (d, J = 5.2 Hz, 1H), 7.16 (dd, J = 5.3, 1.3 Hz, 1H), 7.07 (s, 1H), 4.59 (s, 2H), 3.94–3.89 (m, 3H); consistent with literature.[20]

4.3. Synthesis of bisphosphonate tetraethyl esters

4.3.1. Synthesis of methyl 2-((bis(diethoxyphosphoryl)methyl) amino)isonicotinate (16a)

A 15 mL pressure vessel was charged with the methyl 2-aminoisonicotinate (50 mg, 0.33 mmol), diethyl phosphite (0.25 ml, 2.0 mmol), triethyl orthoformate (0.07 ml, 0.4 mmol) and dissolved in 1 ml toluene. The mixture was stirred at 120 °C overnight. The solution was cooled to room temperature, diluted with ethyl acetate, washed with saturated $NaHCO_3$, brine, dried over $MgSO_4$, filtered and concentrated in vacuo. The residue was purified by silica gel (silica was pre-washed with 0.1% NEt_3 in hexanes/EtOAc 3:1) chromatography on a CombiFlash instrument, using a solvent gradient from 1:3 EtOAc/Hexanes to 100% EtOAc and then to 25%MeOH in EtOAc to give the title compound as an pale yellow powder (106.4 mg, 74%). ^{1}H NMR (400 MHz, $CDCl_3$) δ 8.21 (d, J = 5.2 Hz, 1H), 7.16 (d, J = 5.3 Hz, 1H), 7.10 (s, 1H), 5.51 (td, J = 22.1, 10.1 Hz, 1H), 5.00 (d, J = 10.1 Hz, 1H), 4.26–4.07 (m, 8H), 3.92 (s, 3H), 1.25 (td, J = 7.1, 5.1 Hz, 12H).

^{13}C NMR (75 MHz, CD_3OD) δ 165.58, 130.92, 122.52, 113.55, 110.87, 107.87, δ 63.47 (d, J = 17.7 Hz), 54.46, 44.49 (t, J = 149.9 Hz), 15.90–14.76 (m).

^{31}P NMR (81 MHz, CD_3OD) δ 18.16 (s). MS (ES^{+}) m/z: 461.0 $[M+Na^{+}]^{+}$ ($C_{16}H_{28}N_2NaO_8P_2$).

4.3.2. Synthesis of tetraethyl (((5-bromopyridin-3-yl)amino) methylene)bis (phosphonate) (12)

A 15 mL pressure vessel was charged with the 5-bromopyridin-3-amine (250 mg, 1.44 mmol), diethyl phosphite (1.12 ml, 8.67 mmol), triethyl orthoformate (0.29 ml, 1.73 mmol) and dissolved in 3 ml toluene. Stirred at 80 °C for 18 h, ^{13}P NMR showed only 10% conversion. The reaction was stirred another 14 h at 100 °C. Cooled down and concentrated in vacuo. The residue was purified by silica gel (silica was pre-washed with 0.1% NEt_3 in hexanes/EtOAc 3:1) chromatography on a CombiFlash instrument, using a solvent gradient from 1:3 EtOAc/hexanes to 100% EtOAc and then to 25%MeOH in EtOAc. The product thus obtained was contaminated with ~10% of the mono-phosphonate analog, the mixture was purified by reverse phase chromatography on a CombiFlash instrument using a solvent gradient from 10% CH_3CN/water to 100% CH_3CN. The desired compound was isolated as an off-white powder (290 mg, 44%).

^{1}H NMR (400 MHz, DMSO-d_6) δ 8.26 (s, 1H), 7.85 (s, 1H), 7.59 (s, 1H), 6.44 (d, J = 10.8 Hz, 1H), 4.84 (td, J = 22.8, 10.7 Hz, 1H), 4.16–3.93 (m, 8H), 1.15 (dt, J = 20.7, 7.0 Hz, 12H).

^{13}C NMR (126 MHz, DMSO-d_6) δ 145.31 (t, J = 4.2 Hz), 138.10, 135.62, 121.06, 120.55, 63.08 (dt, J = 17.4, 3.1 Hz), 47.86 (t, J = 144.7 Hz), 16.66 (dt, J = 5.7, 2.8 Hz)

^{31}P NMR (81 MHz, DMSO-d_6) δ 17.22 (s).

MS (ES^{+}) m/z: 459.2 and 461.2 $[M+H^{+}]^{+}$ ($C_{14}H_{26}BrN_2O_6P_2$).

4.4. Examples of Suzuki coupling reactions

A 2 mL microwave reaction vessel was charged with a magnetic stir bar, boronic acid or boronate ester (1.5 equiv), $Pd(PPh_3)_4$ (0.1 equiv) and aryl halide (if a solid); if the aryl halide is an oil, it was added as a solution in 1,4-dioxane via syringe. The reaction vessel was capped with a septum, degassed and flushed with Argon. 1,4-Dioxane was added to bring the concentration of aryl halide to 0.1 M and the mixture was again degassed and flushed with Argon. A solution of 2 M K_2CO_3 (2.5 equiv) was added and the mixture was again degassed and flushed with Argon. The rubber septum was replaced by a Teflon lined seal, under a flow of Argon. The reaction was irradiated to 125 °C for 15–30 min (~40 W), reaction progress was followed by TLC and/or HPLC. The crude was filtered through a plug of Celite, rinsed with 10 mL 1:1 EtOAc/acetone and concentrated under vacuum. The residue was purified by silica gel chromatography (silica was pre-washed with 0.1% Et_3N in hexanes/EtOAc, 3:1 ratio) using a CombiFlash instrument and a solvent gradient from 1:1 EtOAc/hexanes to 100% EtOAc and then to 25% MeOH in EtOAc. The desired product was isolated in yields from 30% to 80% (some examples are given below).

4.4.1. Tetraethyl (((5-phenylpyridin-3-yl)amino)methylene)bis (phosphonate) (13b)

Yield: 34%; as clear, colorless syrup.

^{1}H NMR (400 MHz, DMSO-d_6) δ 8.26 (s, 1H), 8.11 (s, 1H), 7.68 (d, J = 7.1 Hz, 2H), 7.57 (s, 1H), 7.46 (t, J = 7.5 Hz, 2H), 7.38 (d, J = 7.2 Hz, 1H), 6.13 (d, J = 11.0 Hz, 1H), 4.95 (td, J = 22.9, 10.9 Hz, 1H), 4.07 (d, J = 7.0 Hz, 8H), 1.14 (dt, J = 19.3, 7.0 Hz, 11H).

^{13}C NMR (126 MHz, CD_3OD) δ 136.33, 134.20, 128.69, 127.91, 126.70, 118.29, δ 63.61 (d, J = 33.2 Hz), δ 15.29 (d, J = 5.2 Hz).

^{31}P NMR (81 MHz, CD_3OD) δ 20.32 (s).

MS (ES^+) m/z: 479.13 $[M+Na^+]^+$ ($C_{20}H_{30}N_2NaO_6P_2$).

4.4.2. Tetraethyl (((5-(4-isopropoxyphenyl)pyridin-3-yl)amino) methylene) bis(phosphonate) (13f)

Yield: 70%, of pale yellow syrup.

^{1}H NMR (500 MHz, $CDCl_3$) δ 8.25 (s, 1H), 8.05 (d, J = 2.4 Hz, 1H), 7.49–7.44 (m, 2H), 7.13 (s, 1H), 7.00–6.94 (m, 2H), 4.65–4.55 (m, 1H), 4.33–4.10 (m, 9H), 1.37 (d, J = 6.1 Hz, 6H), 1.29 (dt, J = 19.0, 7.1 Hz, 12H).

^{13}C NMR (126 MHz, $CDCl_3$) δ 158.08, 142.30, 138.56, 136.51, 134.75, 129.92, 128.15, 117.77, 116.22, 69.94, δ 63.58 (dd, J = 21.7, 18.6 Hz), 49.88 (t, J = 147.7 Hz), 22.00, 16.39 (dd, J = 6.0, 2.8 Hz).

^{31}P NMR (81 MHz, $CDCl_3$) δ 14.73 (s).

MS (ES^+) m/z: 515.22 $[M+H^+]^+$ ($C_{23}H_{37}N_2O_7P_2$).

4.4.3. Tetraethyl (((5-(4-cyclopropoxyphenyl)pyridin-3-yl)amino) methylene) bis(phosphonate) (13g)

Yield: 99% of pale yellow oil.

^{1}H NMR (500 MHz, $CDCl_3$) δ 8.25 (s, 1H), 8.06 (d, J = 2.4 Hz, 1H), 7.51–7.45 (m, 2H), 7.16–7.11 (m, 3H), 4.30–4.10 (m, 8H), 3.81–3.75 (m, 1H), 1.29 (dt, J = 19.1, 7.1 Hz, 12H), 0.84–0.79 (m, 4H).

^{13}C NMR (126 MHz, $CDCl_3$) δ 159.11, 142.30, 138.63, 136.46, 134.90, 130.55, 128.05, 117.80, 115.49, δ 63.63 (d, J = 36.9 Hz), 50.91, 49.89 (t, J = 147.6 Hz), 16.85–15.63 (m), 6.22.

^{31}P NMR (81 MHz, $CDCl_3$) δ 14.73 (s).

MS (ES^+) m/z: 513.20 $[M+H^+]^+$ ($C_{23}H_{35}N_2O_7P_2$).

4.4.4. Tetraethyl (((5-(3-(cyclopropylcarbamoyl)phenyl)pyridin-3-yl)amino) methylene)bis(phosphonate) (13h)

Yield: 48%; as colorless oil.

^{1}H NMR (400 MHz, acetone-d_6) δ 8.34 (s, 1H), 8.23 (s, 1H), 8.13 (s, 1H), 7.90–7.80 (m, 3H), 7.62 (s, 1H), 7.54 (t, J = 7.7 Hz, 1H), 5.39 (d, J = 10.8 Hz, 1H), 4.67 (td, J = 22.2, 10.4 Hz, 1H), 4.23–4.07 (m, 8H), 2.95 (td, J = 7.3, 3.8 Hz, 1H), 1.23 (dt, J = 18.1, 7.1 Hz, 12H), 0.76 (m, 2H), 0.66–0.60 (m, 2H).

^{13}C NMR (75 MHz, acetone-d_6) δ 167.41, 138.47, 137.24, 136.10, 135.71, 129.49, 128.89, 126.62, 125.68, 117.18, δ 62.89 (d, J = 12.8 Hz), 48.80 (t, J = 145.5 Hz), 23.02, 15.85 (d, J = 2.0 Hz), 5.56.

^{31}P NMR (81 MHz, acetone-d_6) δ 20.62 (s).

MS (ES^+) m/z: 540.3 $[M+H^+]^+$ ($C_{24}H_{36}N_3O_7P_2$).

4.4.5. Tetraethyl (((5-(4-(N-cyclopropylsulfamoyl)phenyl) pyridin-3-yl)amino) methylene)bis(phosphonate) (13i)

Yield: 35%; colorless oil.

^{1}H NMR (400 MHz, acetone-d_6) δ 8.39 (d, J = 2.7 Hz, 1H), 8.28 (d, J = 1.9 Hz, 1H), 7.96 (d, J = 8.7 Hz, 4H), 7.68 (t, J = 2.3 Hz, 1H), 5.44 (d, J = 9.5 Hz, 1H), 4.69 (td, J = 22.1, 10.4 Hz, 1H), 4.23–4.08 (m, 8H), 2.25 (m, 1H), 1.23 (dt, J = 17.4, 7.1 Hz, 12H), 0.56 (m, 4H).

^{13}C NMR (75 MHz, acetone-d_6) δ 143.62, 142.39, 139.99, 137.23, 137.01, 134.60, 127.82, 127.53, 117.07, δ 62.86 (d, J = 11.1 Hz), 48.78 (t, J = 146.0 Hz), 24.19, 15.85 (d, J = 1.8 Hz), 5.17.

^{31}P NMR (81 MHz, acetone-d_6) δ 20.56 (s).

MS (ES^+) m/z: 576.3 $[M+H^+]^+$ ($C_{23}H_{36}N_3O_8P_2S$).

4.4.6. Tetraethyl (((5-(4-(cyclopropanecarboxamido)phenyl) pyridin-3-yl)amino) methylene)bis(phosphonate) (13j)

Yield: 48%; as colorless oil.

^{1}H NMR (400 MHz, acetone-d_6) δ 9.52 (s, 1H), 8.27 (d, J = 2.6 Hz, 1H), 8.20 (d, J = 1.8 Hz, 1H), 7.77 (d, J = 8.7 Hz, 2H), 7.64 (d, J = 8.7 Hz, 2H), 7.55 (s, 1H), 5.27 (d, J = 10.4 Hz, 1H), 4.64 (td, J = 22.1, 10.3 Hz, 1H), 4.22–4.06 (m, 8H), 1.83–1.73 (m, 1H), 1.22 (dt, J = 17.9, 7.1 Hz, 12H), 0.95–0.87 (m, 2H), 0.83–0.75 (m, 2H).

^{13}C NMR (75 MHz, acetone-d_6) δ 171.65, 139.61, 137.04, 135.61, 132.83, 127.19, 119.34, 119.25, 116.53, δ 62.78 (d, J = 12.9 Hz), 48.89 (t, J = 145.0 Hz), 15.83 (d, J = 1.7 Hz), 14.62, 6.80.

^{31}P NMR (81 MHz, acetone-d_6) δ 20.60 (s).

MS (ES^+) m/z: 540.3 $[M+H^+]^+$ ($C_{24}H_{36}N_3O_7P_2$).

4.4.7. Tetraethyl (((4-(4-cyclopropoxyphenyl)pyridin-2-yl) amino) methylene)bis(phosphonate) (7g tetraethyl ester)

Yield: 73%; white solid.

^{1}H NMR (300 MHz, $CDCl_3$) δ 8.09 (d, J = 5.2 Hz, 1H), 7.52 (d, J = 8.6 Hz, 2H), 7.10 (d, J = 8.6 Hz, 2H), 6.83 (d, J = 5.2 Hz, 1H), 6.70 (s, 1H), 5.58 (td, J = 22.2, 9.5 Hz, 1H), 5.01 (d, J = 9.5 Hz, 1H), 4.14–4.21 (m, 8H), 3.90–3.57 (m, 1H), 1.20–1.28 (m, 12H), 0.79 (m, 4H).

^{13}C NMR (75 Hz, $CDCl_3$) δ 159.71, 156.54, 149.33, 147.73, 131.05, 127.86, 115.39, 112.57, 106.33, 63.26–63.48 (m, CH_2), 50.95, 45.09 (t, J = 146.2 Hz, CH), 16.22–16.36 (m, CH_3), 6.24

^{31}P NMR ($CDCl_3$) δ 18.99 ppm.

MS (ES^+) m/z: 513.21 $[M+H^+]^+$ ($C_{23}H_{35}N_2O_7P_2$).

4.5. Synthesis general procedure for amide coupling reactions

To a mixture of 2-((bis(diethoxyphosphoryl)methyl)amino) isonicotinic acid (1 equiv) and amine (1.50 equiv) in a minimal amount of anhydrous DMF were added in sequence: DIPEA (3 equiv) and HATU (1.50 equiv). The reaction was stirred at RT overnight. The reaction mixture was diluted with EtOAc and washed with saturated $NaHCO_3$. The aqueous layer was back-extracted with 4 × 10 ml of EtOAc. All organic layers were combined, washed with brine, dried over anhydrous MgSO4, filtered and concentrated in vacuo. The residue was purified by silica gel (silica was pre-washed with 0.1% NEt_3 in hexanes/EtOAc 3:1) chromatography on a CombiFlash instrument, using a solvent gradient from 1:10 EtOAc/Hexanes to 100% EtOAc and then to 20%MeOH in EtOAc to give the desired amides.

4.5.1. Synthesis of 2-((bis(diethoxyphosphoryl)methyl)amino) isonicotinic acid (16b)

To an ice-cooled solution of methyl 2-((bis(diethoxyphosphoryl)methyl)amino) isonicotinate (50.0 mg, 0.114 mmol) in 1 ml of THF was added 1.0 M LiOH (0.28 ml, 0.285 mmol) and stirred at 0 °C for 1 h. The reaction mixture was then acidified with 1 M HCl and evaporated to dryness under reduced pressure to obtain the free acid. The residue was re-dissolved in EtOAc and washed with water. The aqueous layer was back-extracted with 4 × 10 ml EtOAc. The organic layers were combined, washed with brine, dried over $MgSO_4$, filtered and concentrated in vacuo to give the title compound as a yellow solid (20.6 mg, 43%).

^{1}H NMR (400 MHz, CD_3OD) δ 8.13 (d, J = 3.6 Hz, 1H), 7.27 (s, 1H), 7.11 (d, J = 4.4 Hz, 1H), 5.67 (t, J = 23.5 Hz, 1H), 4.17 (m, 8H), 1.26 (dd, J = 14.7, 7.6 Hz, 12H).

^{31}P NMR (81 MHz, CD_3OD) δ 19.84 (s).

MS (ES^+) m/z: 447.0 $[M+Na^+]^+$ ($C_{15}H_{26}N_2NaO_8P_2$).

4.5.2. Tetraethyl (((4-((4-methoxyphenyl)carbamoyl)pyridin-2-yl)amino)methylene) bis(phosphonate) (10e tetraethyl ester)

Yield: 58% of pale yellow solid.

^{1}H NMR (400 MHz, CD_3OD) δ 8.19 (d, J = 5.3 Hz, 1H), 7.56 (d, J = 9.0 Hz, 2H), 7.16 (s, 1H), 7.05 (d, J = 5.1 Hz, 1H), 6.92 (d, J = 9.0 Hz, 2H), 5.70 (t, J = 23.5 Hz, 1H), 4.27–4.07 (m, 8H), 3.79 (s, 3H), 1.35–1.17 (m, 12H).

^{13}C NMR (75 MHz, CD_3OD) δ 165.58, 157.14, 156.98, 147.50, 144.16, 130.92, 122.52, 113.55, 110.87, 107.87, δ 63.47 (d, J = 17.6 Hz), 54.46, 44.50 (t, J = 150.2 Hz), 15.24 (dd, J = 6.2, 3.1 Hz). ^{31}P NMR (81 MHz, CD_3OD) δ 19.34 (s).

MS (ES^+) m/z: 530.36 $[M+H^+]^+$ ($C_{22}H_{34}N_3O_8P_2$).

4.5.3. Tetraethyl (((4-(isopropylcarbamoyl)pyridin-2-yl)amino) methylene) bis(phosphonate) (10d tetraethyl ester)

Yield: 54%, of beige solid.

^{1}H NMR (300 MHz, CD_3OD) δ 8.13 (d, J = 5.3 Hz, 1H), 7.05 (s, 1H), 6.94 (d, J = 5.2 Hz, 1H), 5.67 (t, J = 23.5 Hz, 1H), 4.27–4.06 (m, 8H), 3.30 (m, 7H), 1.32–1.17 (m, 12H).

^{13}C NMR (75 MHz, CD_3OD) δ 166.51, 157.07, 147.33, 143.93, 110.76, 107.73, δ 63.45 (d, J = 18.2 Hz), 44.47 (t, J = 150.1 Hz), 41.80, 20.99, 15.25 (dd, J = 6.0, 3.0 Hz).

^{31}P NMR (81 MHz, CD_3OD) δ 19.73 (s).

MS (ES^+) m/z: 466.34 $[M+H^+]^+$ ($C_{18}H_{34}N_3O_7P_2$).

4.5.4. Tetraethyl (((4-(phenylcarbamoyl)pyridin-2-yl)amino) methylene) bis(phosphonate) (10b tetraethyl ester)

Yield: 35%, of pale brown oil.

^{1}H NMR (400 MHz, CD_3OD) δ 8.19 (t, J = 5.0 Hz, 1H), 7.66 (t, J = 8.3 Hz, 2H), 7.40–7.32 (m, 2H), 7.19–7.13 (m, 2H), 7.07 (d, J = 5.3 Hz, 1H), 5.71 (t, J = 23.5 Hz, 1H), 4.25–4.13 (m, 8H), 1.27 (t, J = 7.1 Hz, 12H).

^{13}C NMR (75 MHz, CD_3OD) δ 165.44, 157.01, 147.36, 144.02, 130.78, 122.39, 113.41, 110.73, 107.73, δ 63.33 (d, J = 17.7 Hz), 44.36 (t, J = 149.9 Hz), 16.89–13.49 (m).

^{31}P NMR (81 MHz, CD_3OD) δ 19.74 (s).

MS (ES^+) m/z: 500.35 $[M+H^+]^+$ ($C_{21}H_{32}N_3O_7P_2$).

4.6. Tetraethyl (((5-benzylpyridin-3-yl)amino)methylene) bis(phosphonate) (9c tetraethyl ester)

A 2 mL microwave reaction vessel was charged with a magnetic stir bar, tetraethyl (((5-bromopyridin-3-yl)amino)methylene)bis(phosphonate) (50.0 mg, 0.11 mmol), potassium benzyltrifluoroborate (53.9 mg, 0.27 mmol, 2.5 equiv) and $Pd(dppf)Cl_2{\cdot}CH_2Cl_2$ (8.0 mg, 0.01 mmol, 0.1 equiv); capped with a septum, degassed and flushed with Argon. A volume of 1.09 mL 1,4-dioxane was added to bring the concentration of the aryl bromide to 0.1 M, and the mixture was again degassed and flushed with Argon. A solution of 2 M Cs_2CO_3 (0.16 ml, 2.5 equiv) was added and the mixture was again degassed and flushed with Argon. The rubber septum was replaced by a Teflon lined seal, under Argon flow. The reaction was irradiated to 125 °C for 30 min (~40 W), reaction progress was monitored HPLC. After 30 min HPLC analysis showed ~30% conversion, the same amounts of boron reagent, catalyst and base were added to the reaction vessel and irradiation was continued. After another 30 min HPLC analysis showed ~66% conversion, the same amounts boron reagent, catalyst and base were added to the reaction vessel and irradiation was continued. After an additional 30 min, HPLC analysis showed complete conversion. The crude was filtered through a plug of Celite, rinsed with 10 mL 1:1 EtOAc/acetone and concentrated in vacuo. The residue was purified by silica gel (silica was pre-washed with 0.1% NEt_3 in hexanes:EtOAc 3:1) chromatography using a CombiFlash instrument and a solvent gradient from 1:1 EtOAc/hexanes to 100% EtOAc and then to 25% MeOH in EtOAc. The product was isolated as a purple oil in ~75% purity (40 mg). The mixture was purified by preparative HPLC on a Waters Atlantis C18 column using a gradient from 5% CH_3CN/H_2O to 95% with 0.1% formic acid. Fractions of sufficient purity were pooled and lyophilized to dryness, isolated 28 mg (55%) of product as a white, waxy solid.

^{1}H NMR (400 MHz, DMSO-d_6) δ 8.08 (s, 1H), 7.72 (s, 1H), 7.30–7.09 (m, 6H), 5.99 (d, J = 10.6 Hz, 1H), 4.63 (td, J = 22.9, 10.8 Hz, 1H), 4.13–3.86 (m, 8H), 3.79 (s, 2H), 1.09 (dt, J = 23.7, 7.0 Hz, 12H).

^{13}C NMR (126 MHz, DMSO-d_6) δ 143.65, 141.34, 138.65, 136.65, 135.05, 128.99, 128.79, 126.44, 119.18, δ 62.98 (d, J = 21.6 Hz), 48.10 (t, J = 144.6 Hz), 38.74, 16.62, 16.60.

^{31}P NMR (81 MHz, DMSO-d_6) δ 20.180 (s).

MS (ES^+) m/z: 471.33 $[M+H^+]^+$ ($C_{21}H_{33}N_2O_6P_2$).

4.7. Standard procedures for the hydrolysis of the bisphosphonate tetraethyl esters to the diphosphonic acids

A solution of the tetraethyl bisphosphonate ester (1 equiv) in CH_2Cl_2 was cooled to 0 °C and trimethylsilyl bromide (15 equiv) was added *via* syringe. The reaction mixture was stirred at room temperature for 5 days; the completion of conversion was monitored by ^{31}P NMR. The mixture was then concentrated in vacuo, diluted with HPLC grade MeOH (~5 mL), the solvent was evaporated to dryness and this step was repeated four times. The organic solvents were evaporated under vacuum, the residue was suspended in 0.5 mL MeOH, excess water (~5 mL Milli-Q grade) was added to induce full precipitation of the final product. The amorphous powder was collected by filtration, washed with deionized water, twice with HPLC-grade CH_3CN, twice with distilled Et_2O or toluene and dried under vacuum to give the final compound as a solid.

4.7.1. (((4-(4-Cyclopropoxyphenyl)pyridin-2-yl)amino)methylene) diphosphonic acid (7g)

Yield: 93%, as white solid.

^{1}H NMR (500 MHz, D_2O) 7.75 (dd, J = 5.8, 0.6 Hz, 1H), 7.63–7.54 (m, 2H), 7.09–7.01 (m, 2H), 6.82 (d, J = 1.0 Hz, 1H), 6.74 (dd, J = 5.8, 1.6 Hz, 1H), 3.87 (t, J = 19.2 Hz, 1H), 3.77 (hept, J = 1.8 Hz, 1H), 0.67–0.71 (m, 2H), 0.58–0.61 (m, 2H).

^{13}C NMR (125 Hz, D_2O) δ 159.16, 157.84, 149.99, 144.55, 130.81, 128.26, 115.46, 110.28, 105.75, 51.77 (t, J = 122.5 Hz), 51.30, 5.42

^{31}P NMR (81 MHz, D_2O) δ14.04.

HRMS: calcd 399.05110 for ($C_{15}H_{17}N_2O_7P_2$), found (m/z) 399.05093 $[M-H]^-$.

4.7.2. (((5-Phenylpyridin-3-yl)amino)methylene)diphosphonic acid (9b)

Isolated yield: 64%, as a white powder.

^{1}H NMR (500 MHz, D_2O) δ 8.05 (dd, J = 6.0, 2.2 Hz, 2H), 7.80–7.75 (m, 2H), 7.57 (t, J = 7.6 Hz, 2H), 7.52–7.47 (m, 1H), 7.46 (s, 1H), 3.80 (t, J = 19.0 Hz, 2H).

^{13}C NMR (75 MHz, D_2O) δ 137.83, 136.75, 134.14, 133.73, 133.53, 128.98, 128.06, 127.04, 117.68; the Cα was difficult to observe due to coupling with ^{31}P, however, a ^{1}H–^{13}C correlation (δ 1H 3.80 to ^{13}C δ 52.25) was clearly observed in the HSQC spectrum (see supplementary data).

^{31}P NMR (81 MHz, D_2O) δ 14.97 (s).

HRMS m/z: calcd 343.0249 for ($C_{12}H_{13}N_2O_6P_2$), found m/z 343.0251 [M−H$^+$]$^-$.

4.7.3. (((5-benzylpyridin-3-yl)amino)methylene)diphosphonic acid (9c)

Yield: 79%, white powder.

^{1}H NMR (500 MHz, D_2O) δ 7.86 (d, J = 2.5 Hz, 1H), 7.65 (s, 1H), 7.39–7.30 (m, 3H), 7.26 (t, J = 6.7 Hz, 1H), 7.07 (s, 1H), 3.92 (s, 2H), 3.65 (t, J = 19.0 Hz, 1H).^{13}C NMR (126 MHz, D_2O) δ 145.17, 140.97, 137.71, 136.16, 132.55, 128.74, 128.69, 126.34, 120.10, δ 52.10 (t, J = 123.5 Hz), 38.23.

HSQC ^{1}H–^{13}C: δ ^{1}H 3.65 correlates with ^{13}C δ 52.10.

^{31}P NMR (81 MHz, D_2O) δ 15.06 (s).

HRMS: calcd 357.0405 for ($C_{13}H_{15}N_2O_6P_2$), found m/z 357.04149 [M−H]$^-$.

4.7.4. (((5-(4-isopropoxyphenyl)pyridin-3-yl)amino)methylene) diphosphonic acid (9f)

Isolated yield: 71%, as white powder.

^{1}H NMR (500 MHz, D_2O) δ 7.97 (d, J = 2.7 Hz, 1H), 7.96 (d, J = 1.8 Hz, 1H), 7.71–7.66 (m, 2H), 7.38–7.35 (m, 1H), 7.15–7.10 (m, 2H), 4.75 (m, obscured by solvent signal, 1H), 3.74 (t, J = 19.1 Hz, 1H), 1.35 (d, J = 6.1 Hz, 6H).^{13}C NMR (126 MHz, D_2O) δ 156.77, 145.36, 136.20, 133.72, 133.32, 131.07, 128.40, 117.19, 116.80, 71.67, 52.49, 20.99.

HSQC ^{1}H–^{13}C: ^{1}H δ 3.74 correlates with ^{13}C δ 52.49.

^{31}P NMR (81 MHz, D_2O) δ 15.05 (s).

HRMS m/z: calcd 401.0667 for ($C_{15}H_{19}N_2O_7P_2$), found m/z 401.06784 [M−H$^+$]$^-$.

4.7.5. (((5-(4-cyclopropoxyphenyl)pyridin-3-yl)amino)methylene) diphosphonic acid (9g)

27.9 mg, 63%, pale yellow powder.

^{1}H NMR (500 MHz, D_2O) δ 7.83 (d, J = 3.2 Hz, 2H), 7.56 (d, J = 8.8 Hz, 2H), 7.23 (s, 1H), 7.12 (d, J = 8.8 Hz, 2H), 3.87–3.73 (m, 1H), 3.60 (t, J = 19.1 Hz, 1H), 0.77–0.57 (m, 4H).

^{13}C NMR (126 MHz, D_2O) δ 158.13, 145.34, 136.24, 133.79, 133.31, 131.12, 128.26, 117.24, 115.51, δ 52.47 (t, J = 125.3 Hz), 51.26, 5.43.

^{31}P NMR (81 MHz, D_2O) δ 15.06 (s).

HRMS: calcd 399.0511 for ($C_{15}H_{17}N_2O_7P_2$), found m/z 399.05192 [M−H]$^-$.

4.7.6. (((5-(3-(Cyclopropylcarbamoyl)phenyl)pyridin-3-yl)amino) methylene) diphosphonic acid (9h)

Yield: 97%, of a white powder.

^{1}H NMR (400 MHz, D_2O) δ 8.02 (m, 3H), 7.91 (d, J = 8.1 Hz, 1H), 7.77 (d, J = 7.8 Hz, 1H), 7.62 (t, J = 7.8 Hz, 1H), 7.42 (s, 1H), 3.76 (t, J = 19.0 Hz, 1H), 2.84–2.76 (m, 1H), 0.90–0.83 (m, 2H), 0.73–0.67 (m, 2H).

^{13}C NMR (75 MHz, D_2O) δ 172.49, 145.34, 138.29, 136.00, 134.24, 134.10, 134.07, 130.60, 129.29, 126.59, 125.48, 117.54, 22.54, 5.44.

^{31}P NMR (81 MHz, D_2O) δ 15.36 (s).

HRMS: calcd 426.0620 for ($C_{16}H_{18}N_3O_7P_2$), found m/z 426.06280 [M−H]$^-$.

4.7.7. (((5-(4-(*N*-Cyclopropylsulfamoyl)phenyl)pyridin-3-yl) amino)methylene) diphosphonic acid (9i)

Yield: 85%, pale yellow powder.

^{1}H NMR (400 MHz, D_2O) δ 7.97–7.89 (m, 2H), 7.82 (q, J = 8.5 Hz, 4H), 7.32 (s, 1H), 3.62 (t, J = 19.0 Hz, 1H), 2.21–2.12 (m, 1H), 0.45–0.38 (m, 2H), 0.32–0.25 (m, 2H).

^{13}C NMR (75 MHz, D_2O) δ 145.36, 142.82, 137.57, 135.31, 134.66, 134.09, 127.94, 127.44, 117.69, 52.52, 24.23, 4.72.

HSQC ^{1}H–^{13}C: ^{1}H δ 3.62 correlates with ^{13}C δ 53.52.

^{31}P NMR (81 MHz, D_2O) δ 15.38 (s).

HRMS: calcd 462.0290 for ($C_{15}H_{18}N_3O_8P_2S$), found m/z 462.03099 [M−H]$^-$.

4.7.8. (((5-(4-(Cyclopropanecarboxamido)phenyl)pyridin-3-yl) amino)methylene) diphosphonic acid (9j)

Yield: 94%, white powder.

^{1}H NMR (300 MHz, D_2O) δ 7.99 (s, 2H), 7.68 (d, J = 8.5 Hz, 2H), 7.52 (d, J = 8.5 Hz, 2H), 7.40 (s, 1H), 3.76 (t, J = 19.1 Hz, 1H), 1.76 (m, 1H), 0.93 (m, 4H).^{13}C NMR (75 MHz, D_2O) δ 175.95, 145.24, 137.14, 136.05, 134.12, 134.05, 133.56, 127.55, 121.51, 117.43, δ 52.30 (t, J = 124.2 Hz), 14.67, 7.32.

^{31}P NMR (81 MHz, D_2O) δ 15.39 (s).

HRMS: calcd 426.0620 for ($C_{16}H_{18}N_3O_7P_2$), found m/z 426.06265 [M−H]$^-$.

4.7.9. (((4-(Phenylcarbamoyl)pyridin-2-yl)amino)methylene) diphosphonic acid (10b)

Yield: 49%, fine white crystals.

^{1}H NMR (400 MHz, D_2O) δ 7.93 (d, J = 5.4 Hz, 1H), 7.46 (dd, J = 8.5, 1.1 Hz, 2H), 7.38 (dd, J = 10.7, 5.2 Hz, 2H), 7.21 (t, J = 7.4 Hz, 1H), 6.91 (s, 1H), 6.75 (d, J = 5.4 Hz, 1H); central methylene obscured by solvent signal.

^{13}C NMR (75 MHz, D_2O) δ 183.70, 168.57, 158.69, 147.68, 143.62, 136.47, 129.10, 125.97, 122.65, 109.11.

^{31}P NMR (81 MHz, D_2O) δ 14.91.

HRMS: calcd 386.0307 for ($C_{13}H_{14}N_3O_7P_2$), found (m/z) 386.03035 [M−H]$^-$.

4.7.10. (((4-(Isopropylcarbamoyl)pyridin-2-yl)amino)methylene) diphosphonic acid (10d)

Yield: 50%, of pale yellow solid.

^{1}H NMR (400 MHz, D_2O) δ 7.90 (d, J = 5.2 Hz, 1H), 6.74 (s, 1H), 6.65 (d, J = 5.1 Hz, 1H), 4.03 (dt, J = 13.3, 6.6 Hz, 1H), 1.16 (d, J = 6.6 Hz, 6H); central methylene obscured by solvent signal.

^{13}C NMR (75 MHz, D_2O) δ 183.70, 168.91, 158.64, 147.43, 143.80, 108.90, 42.34, 21.09.

^{31}P NMR (81 MHz, D_2O) δ 14.93.

HRMS: calcd 352.0463 for ($C_{10}H_{16}N_3O_7P_2$), found (m/z) 352.04775 [M−H]$^-$.

4.7.11. (((4-((4-Methoxyphenyl)carbamoyl)pyridin-2-yl)amino) methylene) diphosphonic acid (10e)

Yield: 86%, fine yellow solid.

^{1}H NMR (400 MHz, D_2O) δ 7.91 (d, J = 5.2 Hz, 1H), 7.35 (d, J = 9.0 Hz, 2H), 6.93 (d, J = 9.0 Hz, 2H), 6.88 (s, 1H), 6.73 (d, J = 5.3 Hz, 1H), 3.73 (s, 3H); central methylene obscured by solvent.

^{13}C NMR (75 MHz, D_2O) δ 183.70, 168.59, 158.83, 156.72, 147.70, 143.48, 129.73, 124.57, 114.34, 108.87, 55.41.

^{31}P NMR (81 MHz, D_2O) δ 14.92.

HRMS: calcd 416.0413 for ($C_{14}H_{16}N_3O_8P_2$), found m/z 416.04136 [M−H]$^-$.

References and notes

1. Berndt, N.; Hamilton, A. D.; Sebti, S. M. *Nat. Rev.* **2011**, *11*, 775.
2. Rondeau, J. M.; Bitsch, F.; Bourgier, E.; Geiser, M.; Hemmig, R.; Kroemer, M.; Lehmann, S.; Ramage, P.; Rieffel, S.; Strauss, A.; Green, J. R.; Jahnke, W. *ChemMedChem* **2006**, *1*, 267.
3. Kavanagh, K. L.; Guo, K.; Dunford, J. E.; Wu, X.; Knapp, S.; Ebetino, F. H.; Rogers, M. J.; Russell, G. G.; Oppermann, U. *Proc. Natl. Acad. Sci. U.S.A.* **2006**, *103*, 7829.
4. Mönkkönen, H.; Auriola, S.; Lehenkari, P.; Kellinsalmi, M.; Hassinen, I. E.; Vepsäläinen, J.; Mönkkönen, J. *Br. J. Pharmacol.* **2006**, *147*, 437.
5. Mitrofan, L. M.; Pelkonen, J.; Mönkkönen, J. *Bone* **2009**, *45*, 1153.
6. Naoe, M.; Ogawa, Y.; Takeshita, K.; Morita, J.; Shichijo, T.; Fuji, K.; Fukagai, T.; Iwamoto, S.; Terao, S. *Oncol. Res.* **2010**, *18*, 493.
7. Gnant, M.; Mlineritsch, B.; Schippinger, W.; Luschin-Ebengreuth, G.; Pöstlberger, S.; Menzel, C.; Jakesz, R.; Seifert, M.; Hubalek, M.; Bjelic-Radisic, V.; Samonigg, H.; Tausch, C.; Eidtmann, H.; Steger, G.; Kwasny, W.; Dubsky, P.; Fridrik, M.; Fitzal, F.; Stierer, M.; Rücklinger, E.; Greil, R. *N. Engl. J. Med.* **2009**, *360*, 679.
8. Almubarak, H.; Jones, A.; Chaisuparat, R.; Zhang, M.; Meiller, T. F.; Scheper, M. A. *J. Carcinog.* **2011**, *10*, 1.
9. Morgan, G. J.; Davies, F. E.; Gregory, W. M.; Cocks, K.; Bell, S. E.; Szubert, A. J.; Navarro-Coy, N.; Drayson, M. T.; Owen, R. G.; Feyler, S.; Ashcroft, A. J.; Ross, F.; Byrne, J.; Roddie, H.; Rudin, C.; Cook, G.; Jackson, G. H.; Child, J. A. *Lancet* **1989**, *2010*, 376.
10. Chapman, M. A.; Lawrence, M. S.; Keats, J. J.; Cibulskis, K.; Sougnez, C.; Schinzel, A. C.; Harview, C. L.; Brunet, J. P.; Ahmann, G. J.; Adli, M.; Anderson, K. C.; Ardlie, K. G.; Auclair, D.; Baker, A.; Bergsagel, P. L.; Bernstein, B. E.; Drier, Y.; Fonseca, R.; Gabriel, S. B.; Hofmeister, C. C.; Jagannath, S.; Jakubowiak, A. J.; Krishnan, A.; Levy, J.; Liefeld, T.; Lonial, S.; Mahan, S.; Mfuko, B.; Monti, S.; Perkins, L. M.; Onofrio, R.; Pugh, T. J.; Rajkumar, S. V.; Ramos, A. H.; Siegel, D. S.; Sivachenko, A.; Stewart, A. K.; Trudel, S.; Vij, R.; Voet, D.; Winckler, W.; Zimmerman, T.; Carpten, J.; Trent, J.; Hahn, W. C.; Garraway, L. A.; Meyerson, M.; Lander, E. S.; Getz, G.; Golub, T. R. *Nature* **2011**, *471*, 467.
11. Morita, C. T.; Jin, C.; Sarikonda, G.; Wang, H. *Immunol. Rev.* **2007**, *215*, 59.
12. Li, J.; Herold, M. J.; Kimmel, B.; Müller, I.; Rincon-Orozco, B.; Kunzmann, V.; Herrmann, T. *J. Immunol.* **2009**, *182*, 8118.
13. Kunzmann, V.; Bauer, E.; Wilhelm, M. *N. Engl. J. Med.* **1999**, *340*, 737.
14. Zhang, Y.; Cao, R.; Yin, F.; Lin, F.-Y.; Wang, H.; Krysiak, K.; No, J.-H.; Mukkamala, D.; Houlihan, K.; Li, J.; Morita, C. T.; Oldfield, E. *Angew. Chem., Int. Ed.* **2010**, *49*, 1136.
15. Zhang, Y.; Cao, R.; Yin, F.; Hudock, M. P.; Guo, R.-T.; Krysiak, K.; Mukherjee, S.; Gao, Y.-G.; Robinson, H.; Song, Y.; No, J. H.; Bergan, K.; Leon, A.; Cass, L.; Goddard, A.; Chang, T.-K.; Lin, F.-Y.; Van Beek, E.; Papapoulos, S.; Wang, A. H.-J.; Kudo, T.; Ochi, M.; Mukkamala, D.; Oldfield, E. *J. Am. Chem. Soc.* **2009**, *131*, 5153.
16. Dunford, J. E. *Curr. Pharm. Des.* **2010**, *16*, 2961.
17. Lin, Y.-S.; Park, J.; De Schutter, J. W.; Huang, X. F.; Berghuis, A. M.; Sebag, M.; Tsantrizos, Y. S. *J. Med. Chem.* **2012**, *55*, 3201.
18. Molander, G. A.; Ito, T. *Org. Lett.* **2001**, *3*, 393.
19. Lorenz, J. C.; Long, J.; Yang, Z.; Xue, S.; Xie, Y.; Shi, Y. *J. Org. Chem.* **2004**, *69*, 327.
20. Yin, J.; Xiang, B.; Huffman, M. A.; Raab, C. E.; Davies, I. W. *J. Org. Chem.* **2007**, *72*, 4554.
21. De Schutter, J. W.; Zaretsky, S.; Welbourn, S.; Pause, A.; Tsantrizos, Y. S. *Biorg. Med. Chem. Lett.* **2010**, *20*, 5781.
22. Dunford, J. E.; Kwaasi, A. A.; Rogers, M. J.; Barnett, B. L.; Ebetino, F. H.; Russell, R. G. G.; Oppermann, U.; Kavanagh, K. L. *J. Med. Chem.* **2008**, *51*, 2187.
23. Rappoport, Z. *The chemistry of the cyclopropyl group*; Wiley: Chichester; New York, 1987.
24. Gagnon, A.; Duplessis, M.; Fader, L. *Org. Prep. Proced. Int.* **2010**, *42*, 1.
25. Tsuzuki, S.; Honda, K.; Uchimaru, T.; Mikami, M.; Fujii, A. *J. Phys. Chem. A* **2006**, *110*, 10163.
26. Ran, J.; Wong, M. W. *J. Phys. Chem. A* **2006**, *110*, 9702.